Theoretical Rotation, Pseudorotation, and Pseudoinversion Barriers for the Hydroxyphosphoranyl Radical†

Christopher J. Cramer

U.S. Army Chemical Research Development and Engineering Center, Research Directorate, Physics Division, Chemometric and Biometric Modeling Branch, Aberdeen Proving Ground, Maryland 21010-5423. *Received March 23, 1990*

Abstract: Hydroxyphosphoranyl, $H_3POH^•$, has been studied computationally and found to have two local minimum equilibrium structures. Each is characterized by a trigonal-bipyramidal geometry in which the unpaired electron is localized equatorially. They differ in the disposition of the hydroxyl group, either axial (preferred) or equatorial. All possible transition states for the permutation of any number of substituents have been located and characterized at the MP2/6-31G*//6-31G* + ZPVE level. Pseudorotation intermediates were found to have trigonal-bipyramidal geometries in which the unpaired electron is localized axially. Pseudorotations permuting only hydrogen atoms had barriers of 4–10 kcal/mol. Interconversion of the two local minima for $H_3POH^•$ was found to be accomplished more efficiently by a pseudoinversion process (14.9 kcal/mol) than a pseudorotation (17.0 kcal/mol). Analysis of the distribution of spin density in $H_3POH^•$ is provided and arguments about the controversial geometries of two other phosphoranyl radicals are analyzed therewith.

Tetrasubstituted, open-shell phosphorus compounds, termed phosphoranyl radicals, were first proposed as metastable reaction intermediates in 1957.[1,2] The kinetics of their formation, typically from addition of simple radicals to phosphines or phosphites, and of their decomposition have been studied[3] with special attention paid to stereochemical issues involved.[4] These arise from consideration of the various trigonal-bipyramidal (TBP) geometries available to the phosphoranyl radical, viewing the "unpaired" electron as a fifth substituent (Chart I). Facile permutational isomerism is generally noted for phosphoranyl radicals in the absence of such constraints as inclusion of the phosphorus atom in small ring systems.[4,5] Since bond formation (and its microscopic reverse, bond scission) is postulated to occur apically,[6] permutational isomerism is a requirement for observation of net overall substitution at phosphorus by an addition/elimination sequence. A variety of discrete, permutational processes has been proposed for TBP systems; these will be individually treated in detail in the discussion.

Electron spin resonance spectroscopy has proven to be particularly useful in establishing the structures and permutational kinetics for a variety of phosphoranyl radicals.[7] With regard to structure, it has been observed that the vast majority of these species prefer the TBP_e geometry.[8] Others, which possess very low lying σ^*_{P-X} orbitals, have been proposed to adopt distorted tetrahedral (DT) geometries in which the unpaired electron localizes primarily in a P–X antibonding orbital (Chart I).[9] Proposals for TBP_a structures based on both ESR and X-ray crystal studies have appeared,[10] giving rise to at times heated controversy[11] over the relative preference for TBP_e or DT structures compared to TBP_a.

In contrast to the large body of spectroscopic and preparative experimental work, theory has focused scant attention on phosphoranyl radicals. Phosphoranyl itself, $PH_4^•$, has seen the most study.[12-14] However, ab initio efforts concerned with its permutational isomerism have been characterized by small basis sets (often lacking d orbitals on phosphorus!), incomplete geometry optimizations, and failure to account for correlation effects.[13] In addition to $PH_4^•$, the complete series of fluorophosphoranyl radicals ($H_nF_{4-n}P^•$, n = 0–3) has been studied at similar[13a,b] and higher[13c] levels of theory. Although hyperfine coupling constants (hfs) for these systems have been predicted by ab initio and semiempirical methods,[14] they are not particularly well correlated, either between methods or with experiment. Nevertheless, these studies are often invoked with ESR results from widely different phosphoranyl species as proof of a postulated geometry—a practice that must be regarded with some skepticism.

Our own interest in phosphoranyl radicals arises from their potential intermediacy in the breakdown of environmentally toxic organophosphorus compounds.[15] These particular molecules are

† Part 3 in the series Computational Studies of Open-Shell Phosphorus Oxyacids.

(1) Ramirez, F.; McElvie, N. *J. Am. Chem. Soc.* **1957**, *79*, 5929.
(2) Reviews: (a) Bentrude, W. G. *Acc. Chem. Res.* **1982**, *15*, 117. (b) Roberts, B. P. In *Advances in Free Radical Chemistry*; Williams, G. H., Ed.; Heyden and Sons: London, 1980; Vol. 6, p 225.
(3) (a) Bentrude, W. G. In *Organic Free Radicals*; Pryor, W. A., Ed.; ACS Symposium Series 69; American Chemical Society: Washington DC, 1978; Chapter 20. (b) Roberts, B. P.; Scaiano, J. C. *J. Chem. Soc., Perkin Trans. 2* **1981**, 905. (c) Griller, D.; Ingold, K. U.; Patterson, L. K.; Scaiano, J. C.; Small, R. D., Jr. *J. Am. Chem. Soc.* **1979**, *101*, 3780. (d) Kryger, R. G.; Lorand, J. P.; Stevens, N. R.; Herron, N. R. *Ibid.* **1977**, *99*, 7589.
(4) (a) Cooper, J. W.; Roberts, B. P. *J. Chem. Soc., Perkin Trans. 2* **1977**, 730. (b) Bentrude, W. G.; Hargis, J. H.; Johnson, N. A.; Min, T. B.; Rusek, P. E., Jr.; Tan, H. W.; Wielesek, R. A. *J. Am. Chem. Soc.* **1976**, *98*, 5348.
(5) (a) Baban, J. A.; Roberts, B. P. *J. Chem. Soc., Perkin Trans. 2* **1980**, 876. (b) Elson, I. H.; Parrott, M. J.; Roberts, B. P. *J. Chem. Soc., Chem. Commun.* **1975**, 586. (c) Krusic, P. J.; Meakin, P. *Chem. Phys. Lett.* **1973**, *18*, 347. (d) Griller, D.; Ingold, K. U. *J. Am. Chem. Soc.* **1975**, *97*, 1813. (e) Nakanishi, A.; Nishikida, K.; Bentrude, W. G. *Ibid.* **1978**, *100*, 6398, 6403.
(6) (a) Hay, R. S.; Roberts, B. P. *J. Chem. Soc., Perkin Trans. 2* **1978**, 770. (b) Cooper, J. W.; Roberts, B. P. *J. Chem. Soc., Chem. Commun.* **1977**, 228. (c) Lohr, L. L.; Boehm, R. C. *J. Phys. Chem.* **1987**, *91*, 3203. (d) Lohr, L. L. *Ibid.* **1984**, *88*, 5569.
(7) For a review of the earlier literature, see: Schipper, P.; Jansen, E. H. J. M.; Buck, H. M. *Top. Phosphorus Chem.* **1977**, *9*, 407.
(8) (a) PH_4: Colussi, A. J.; Morton, J. R.; Preston, K. F. *J. Chem. Phys.* **1975**, *62*, 2004. (b) PF_4: Fessenden, R. W.; Schuler, R. H. *Ibid.* **1966**, *45*, 1845. (c) PCl_4: Kokoszka, G. F.; Brinkman, F. E. *J. Am. Chem. Soc.* **1970**, *92*, 1199. (d) $POCl_3^-$: Gilibro, T.; Williams, F. *Ibid.* **1974**, *96*, 6032. (e) $ROPH_3$: Krusic, P. J.; Mahler, W.; Kochi, J. K. *Ibid.* **1972**, *94*, 6033. (f) $(RO)Cl_2PO^-$: Nelson, D. J.; Symons, M. C. R. *J. Chem. Soc., Dalton Trans.* **1974**, 1164.
(9) (a) Hay, R. S.; Roberts, B. P.; Singh, K.; Wilkinson, J. P. T. *J. Chem. Soc., Perkin Trans. 2* **1979**, 756. (b) Baban, J. A.; Cooksey, C. J.; Roberts, B. P. *Ibid.* **1979**, 781. (c) Boekestein, G.; Jansen, E. H. J. M.; Buck, H. M. *J. Chem. Soc., Chem. Commun.* **1974**, 118.
(10) (a) Hamerlinck, J. H. H.; Schipper, P.; Buck, H. M. *J. Am. Chem. Soc.* **1983**, *105*, 385. (b) Hamerlinck, J. H. H.; Schipper, P.; Buck, H. M. *Ibid.* **1980**, *102*, 5679. (c) Hamerlinck, J. H. H.; Schipper, P.; Buck, H. M. *J. Org. Chem.* **1983**, *48*, 306. (d) Hamerlinck, J. H. H.; Schipper, P.; Buck, H. M. *J. Chem. Phys.* **1982**, *76*, 2161.
(11) Roberts, B. P. *Tetrahedron Lett.* **1983**, 3377.
(12) Demolliens, A.; Eisenstein, O.; Huberty, P. C.; Lefour, J. M.; Ohanessian, G.; Shaik, S. S.; Velatron, F. *J. Am. Chem. Soc.* **1989**, *111*, 5623.
(13) (a) Janssen, R. A. J.; Visser, G. J.; Buck, H. M. *J. Am. Chem. Soc.* **1984**, *106*, 3429. (b) Howell, J. M.; Olsen, J. F. *Ibid.* **1976**, *98*, 7119. (c) Cramer, C. J. *Ibid.*, submitted for publication.
(14) (a) Bischof, P.; Friedrich, G. *J. Comput. Chem.* **1982**, *3*, 486. (b) VanDijk, J. M. I.; Pennings, J. F. M.; Buck, H. M. *J. Am. Chem. Soc.* **1975**, *97*, 4836. (c) Penkovskii, V. V. *Dokl. Akad. Nauk. SSSR* **1978**, *243*, 375. (d) Colussi, A. J.; Morton, J. R.; Preston, K. F. *J. Phys. Chem.* **1975**, *79*, 1855. (e) Weber, J.; Geoffrey, M. *Theor. Chim. Acta* **1977**, *43*, 299.
(15) (a) Cramer, C. J.; Famini, G. R. *J. Am. Chem. Soc.* **1990**, *112*, 5460. (b) Loo, S. H.; Peters, N. K.; Frost, J. W. *Biochem. Biophys. Res. Commun.* **1987**, *148*, 148. (c) Avila, L. Z.; Loo, S. H.; Frost, J. W. *J. Am. Chem. Soc.* **1987**, *109*, 6758. (d) Frost, J. W.; Loo, S.; Cordeiro, M. L.; Li. D. *Ibid.* **1987**, *109*, 2166. (e) Cordeiro, M. L.; Pompliano, D. L.; Frost, J. W. *Ibid.* **1986**, *108*, 332.

Chart I

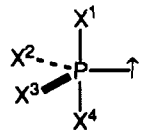

Trigonal bipyramid with free electron equatorial (TBP_e)

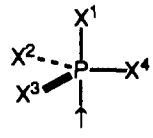

Trigonal bipyramid with free electron apical/axial (TBP_a)

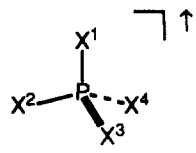

Distorted tetrahedron with free electron in apical σ* orbital (DT)

Table I. Relative Energies of Conformational Isomers of **1**–**7** at Various Theoretical Levels

	relative energy, kcal/mol			
	6-31G*//3-21G(*)		MP2/6-31G*//	imaginary
structure	UHF[a]	UMP2[b]	6-31G* + ZPVE[c]	frequency,[c] cm^{-1}
1a	0.4 *0.2*	0.4 *0.5*	0.7	214.1*i*
1b[d]	0.0 *0.0*	0.0 *0.0*	0.0	none
1c	4.0 *4.7*	4.6 *5.9*	*e*	*e*
1d	4.2 *4.7*	5.2 *6.3*	4.6	34.6*i*
2a	9.8 *9.6*	11.8 *11.6*	10.4	350.6*i*
2b	4.9 *4.4*	6.0 *5.4*	5.8	none
2c	10.1 *9.4*	12.4 *11.9*	11.0	443.3*i*
3a	12.4 *14.7*	13.3 *16.3*	12.0	633.5*i*
3b	13.6 *16.0*	14.4 *17.6*	12.7	686.8*i*
4a	7.0 *6.3*	4.6 *4.1*	4.3	559.0*i*
4b	11.2 *10.8*	9.5 *9.5*	9.0	539.0*i*
5a	18.2 *16.8*	19.5 *17.4*	17.0	1131.3*i*
5b	19.6 *18.0*	21.3 *19.2*	18.8	1093.8*i*
6a	18.5 *19.2*	15.3 *16.4*	14.9	1349.0*i*
6b	23.6 *23.7*	22.4 *22.8*	22.6	808.9*i*
7a	5.7 *5.9*	8.6 *8.3*	4.4	none
7b	5.8 *5.1*	9.2 *8.1*	5.0	none

[a] Relative energies for structures optimized fully at the given level with respect to symmetry constraints except for **1c**, which was constrained to ωHPOH = 0°. [b] Relative energies for single-point calculations done at the HF-optimized geometries of the basis set employed. [c] Frequency calculations were performed at the 6-31G*//6-31G* level and ZPVE energies scaled by 0.89. [d] Absolute energies: UHF/3-21G(*), −415.781 30 au; UHF/6-31G*, −417.821 49 au; UMP2/3-21G(*), −416.016 61 au; UMP2/6-31G*, −418.121 35 au. [e] Not a stationary point.

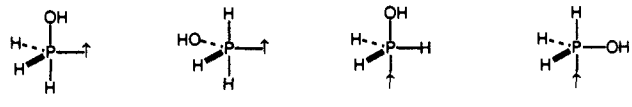

1 **2** **3** **4**

Figure 1. The four structures available to hydroxyphosphoranyl by permuting the locations of the hydroxyl group and the unpaired electron within a trigonal-bipyramidal geometry.

often substituted with alkoxyl or hydroxyl groups. We are particularly concerned with the electronic effects introduced by these ligands which, unlike the hydrogen or fluorine substituents heretofore studied, have internal dipoles and relatively lower symmetry. Thus, as a first-order model to more complex, oxygenated phosphoranyl radicals, we have examined the conformational hypersurface for hydroxyphosphoranyl, $H_3POH^{\bullet}$.

Computational Methods

All structures were fully optimized at both the UHF/3-21G(*)[16] and UHF/6-31G*[17] levels of theory. Correlation effects were accounted for at the UMP2 level[18] with core orbitals included in the perturbation treatment. Analytic harmonic frequency computations were performed for all stationary points at the 6-31G* level. Frequencies were scaled by 0.89 when calculating zero-point vibrational energies (ZPVE).[19a] Calculations were performed on a Local Area Vax Cluster employing the Gaussian 82 suite of programs.[20] Geometry optimizations employed the tight convergence criteria option available in the package in order to improve the quality of the analytic frequency calculations.

Results

Within the constraint of trigonal-bipyramidal geometry and ignoring hydroxyl rotamers, the unique hydroxyl group and unpaired electron generate four possible stereostructures (Figure 1). These are **1**, hydroxyl axial, unpaired electron equatorial; **2**, hydroxyl equatorial, unpaired electron equatorial; **3**, hydroxyl axial, unpaired electron axial; and **4**, hydroxyl equatorial, unpaired electron axial. Explicit consideration of the rotameric forms derived from the hydroxyl group will in general produce structures of C_1 symmetry. In a few cases where coplanarity of the hydroxyl group, any one hydrogen, and the main axis of the singly occupied orbital is achieved, structures of C_s symmetry arise. For convenience throughout in conformationl descriptions, the unpaired electron, which cannot be classically localized, will be considered to be a point substituent. When equatorial, it will be assumed to lie on the bisector of the X^1_e–P–X^2_e angle, and when axial, it will be assumed to lie on the P–X_a axis, where X_e and X_a are, respectively, equatorially and axially disposed substituent atoms attached to phosphorus.

For **1**, four distinct rotamers were calculated. In **1a** the hydroxyl group eclipses the unpaired electron (C_s, dihedral = 0°), in **1b** it is gauche to it (C_1, dihedral = 50°), in **1c** the hydroxyl group was constrained to eclipse a P–H_e bond [C_1 (constrained), dihedral = 128°], and in **1d** the hydroxyl proton is antiperiplanar to the unpaired electron (C_s, dihedral = 180°). Some geometrical details for these structures may be found in Figure 2 and relative energies are collected in Table I. Vibrational analysis indicates **1a** and **1d** to be transition states with imaginary frequencies of 214*i* and 35*i*, respectively. The very small magnitude of these imaginary frequencies indicates that the local hypersurface is quite flat in these regions in the direction of the negative normal mode. Structure **1c** is not a stationary point and converges smoothly to local minimum **1b** when unconstrained. Figure 3 presents these rotational results graphically.

For structure **2**, three rotamers were calculated. In **2a**, the hydroxyl group eclipses the unpaired electron (C_s, dihedral = 0°), in **2b** it essentially eclipses an axial P–H bond (C_1, dihedral = 91°), and in **2c** it eclipses the equatorial P–H bond (C_s, dihedral = 180°). Geometries and relative energies are again collected in Figure 2 and Table I, respectively. Vibrational analysis indicates **2a** and **2c** to be transition states (imaginary frequencies of 351*i* and 443*i*, respectively) while **2b** is a local minimum. The graphically portrayed rotation coordinate may be found in Figure 3.

For structure **3**, the two C_s structures resulting from location of the hydroxyl proton antiperiplanar to P–H_e, **3a**, and hydroxyl eclipsing P–H_e, **3b**, were calculated. Vibrational analysis indicates them both to be transition states (imaginary frequencies of 634*i* and 687*i*, respectively). Relaxation of C_s symmetry by some P–O bond rotation invariably gave structures that smoothly converged to **2b**. A similar situation was noted for **4**. The two C_s structures resulting from hydroxyl eclipsing the unpaired electron, **4a**, and the axial P–H bond, **4b**, were both found to be transition states (imaginary frequencies of 559*i* and 539*i*, respectively). Here, symmetry-relaxed structures converged smoothly to **1b**. Two other C_s TBP_a transition states bearing a gross resemblance to **4a** and

(16) Pietro, W. S.; Francl, M. M.; Hehre, W. J.; DeFrees, D. J.; Pople, J. A.; Binkley, J. S. *J. Am. Chem. Soc.* **1982**, *104*, 5039.
(17) Francl, M. M.; Pietro, W. J.; Hehre, W. J.; Binkley, J. S.; Gordon, M. S.; DeFrees, D. J.; Pople, J. A. *J. Chem. Phys.* **1982**, *77*, 3654.
(18) Moller, C.; Plesset, M. S. *Phys. Rev.* **1934**, *46*, 618.
(19) (a) Hehre, W. J.; Radom, L.; Schleyer, P. v. R.; Pople, J. A. *Ab Initio Molecular Orbital Theory*; Wiley: New York, 1986. (b) Dykstra, C. E. *Ab Initio Calculation of the Structures and Properties of Molecules*, Elsevier: Amsterdam, 1988. (c) Szabo, A.; Ostlund, N. S. *Modern Quantum Chemistry*; Macmillan: New York, 1982.
(20) Binkley, J. S.; Frisch, M. J.; DeFrees, D. J.; Raghavachari, K.; Whiteside, R. A.; Schlegel, H. B.; Fleuder, E. M.; Pople, J. A. *Gaussian 82* (release H version); Carnegie-Mellon University: Pittsburgh, PA, 1983.

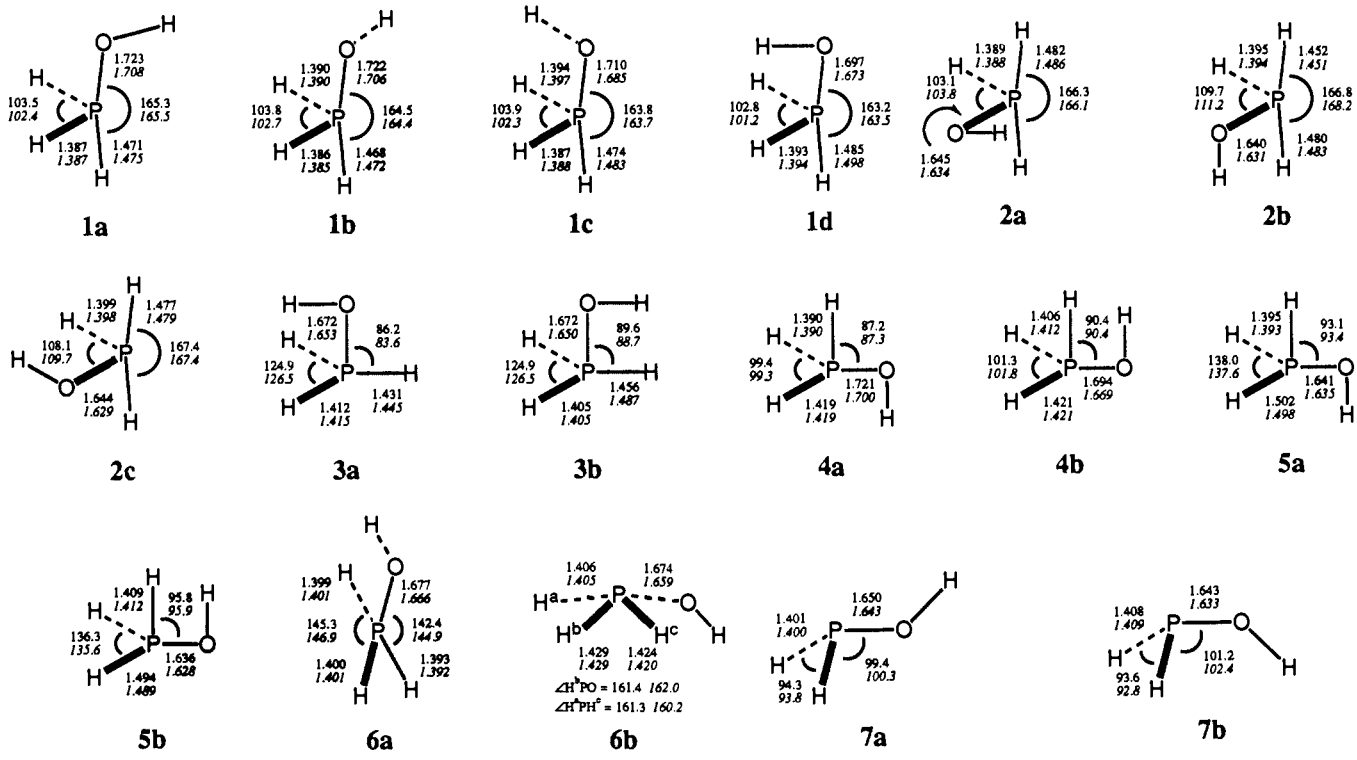

Figure 2. Selected geometrical parameters for structures **1**–**7** found at the UHF/6-31G* level. Values in italics were found at the 3-21G(*) level. Bond lengths are in angstroms, bond angles in degrees.

4b were also found, with imaginary frequencies of 1131*i* and 1094*i*. However, relaxation of these structures could lead to *either* **1b** or **2b**, depending upon the direction of the geometrical perturbation imposed to break symmetry. For ease of discussion, they will be referred to as **5a** and **5b**, respectively.

In addition, two structures were found in which the phosphoranyl compound adopts a geometry other than trigonal bipyramidal. The first, **6a**, is a transition state (C_1, imaginary frequency 1349*i*) with a geometry intermediate between square planar and tetrahedral. The second, **6b**, is a transition state (C_s, imaginary frequency 809*i*) approximately midway between square planar and square pyramidal in geometry.

Finally, for comparative purposes, phosphinous acid was calculated in the presence of a hydrogen atom (10-Å separation) in both its anti, **7a**, and syn, **7b** forms.[21] Relative energies and geometries for structures **3**–**7** may again be found in Table I and Figure 2. For **3a**, **4a**, **5a**, **6a**, and **6b**, detailed pseudo-three-dimensional structures together with the displacement vectors corresponding to the negative normal mode are presented in Figure 4.

Discussion

Theoretical Models. Prior to analysis of the conformational tendencies of hydroxyphosphoranyl, it is appropriate to make some comparison between the various levels of theory employed for this system. Relative energies calculated at the UHF/3-21G(*) level compare well with those obtained at UHF/6-31G*, the average absolute deviation being 10.9%. (It is noteworthy that the deviation is always negative for phosphoranyl structures having an equatorial hydroxyl and positive for those having an axial hydroxyl.) There is, furthermore, no evidence of increasing spin contamination from higher multiplicity states with the smaller basis set; for both basis sets, $\langle S^2 \rangle$ fell between 0.75 and 0.78 for all structures. In addition, although it is well established that the effectivness of post-Hartree–Fock methods is dependent upon the quality of the underlying basis,[19] the average absolute deviation of the UMP2/3-21G(*) results from the UMP2/6-31G* is 11.2%—a mere 0.3% increase from the UHF value.

With respect to predicted geometries, the 3-21G(*) level fares poorly with the P–O bond length, consistently underestimating it by 0.02–0.03 Å relative to 6-31G*. Since Hartree–Fock methods inherently tend to underestimate bond length,[19] this deviation is presumably in the incorrect direction. Axial P–H bond lengths are treated more consistently, with average *over*estimations of less than 0.01 Å, while equatorial P–H bond lengths are usually within 0.001 Å. The X^1_a–P–X^2_a bond angle found for **1** and **2** at the 6-31G* level is consistently reproduced at 3-21G(*) (average absolute deviation of 0.3°) while the agreement for other angles is fair (average absolute deviation of ~1.0°).

With respect to electron correlation, it is apparent that even the UMP2 level captures significant effects. With both bases, the energies relative to global minimum **1b** of structures **1**, **2**, **3**, **5**, and **7** increase by 10–50%, while those of structures **4** and **6** decrease by a similar margin.

Given the above observations, it appears that for phosphoranyl radicals substituted with so many heavy atoms that use of the 6-31G* basis becomes impractical, calculations at the 3-21G(*) level will still be of value. For the remainder of the discussion, all energies referred to will be from UMP2/6-31G*//6-31G* + ZPVE calculations (Table I).[22]

Rotation Barriers. While it is unsurprising that the minimum energy conformation in **1** places the O–H bond gauche to the unpaired electron, the 3-fold barrier predicted by assuming bond-eclipsed conformers to be local maxima on the rotation coordinate fails to emerge (Figure 3). Thus, although eclipsing of the unpaired electron does indeed generate a very low energy local maximum, eclipsing of an equatorial P–H bond in **1c** does

(21) Phosphinous acid has seen extensive computational study. The relative energy ordering of these two rotameric local minima is quite dependent on basis set. This current theoretical treatment appears to be the highest level to date where both are considered. See: (a) Nguyen, M. T.; Hegarty, A. F. *J. Chem. Soc., Perkin Trans. 2* **1987**, *47*, and references cited therein. (b) Cramer, C. J.; Dykstra, C. E.; Denmark, S. E. *Chem. Phys. Lett.* **1987**, *136*, 17. (c) Person, W. B.; Kwiatkowski, J. S.; Bartlett, R. J. *J. Mol. Struct.* **1987**, *157*, 237. (d) Magnusson, E. *Aust. J. Chem.* **1986**, *39*, 735. (e) Schmidt, M. W.; Gordon, M. S. *J. Am. Chem. Soc.* **1985**, *107*, 1922. (f) Wallmeier, H.; Kutzelnigg, W. *J. Am. Chem. Soc.* **1979**, *101*, 2804.

(22) Others have performed far more exhaustive analysis of basis set effects in hypervalent phosphorus; see, for instance: (a) Streitwieser, A., Jr.; Rajca, A.; McDowell, R. S.; Glaser, R. *J. Am. Chem. Soc.* **1987**, *109*, 4184. (b) Rajca, A.; Rice, J. E.; Streitwieser, A., Jr.; Schaefer, H. F., III *Ibid.* **1987**, *109*, 4189. (c) Keil, F.; Kutzelnigg, W. *Ibid.* **1975**, *97*, 3622.

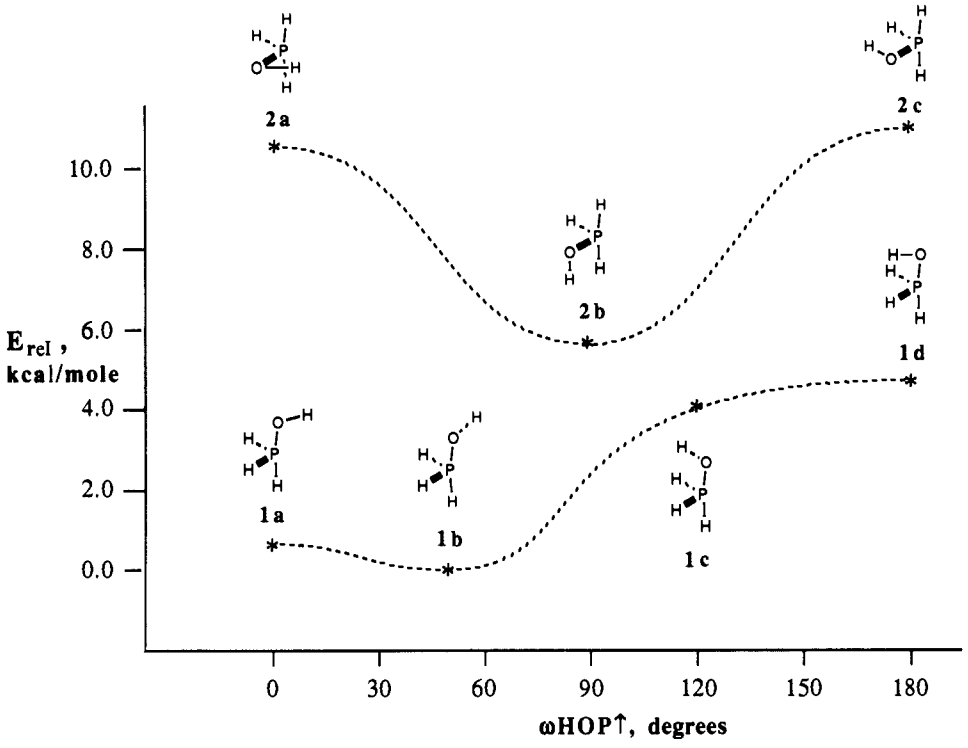

Figure 3. Rotational dynamics for the hydroxyl group in structures **1** and **2**.

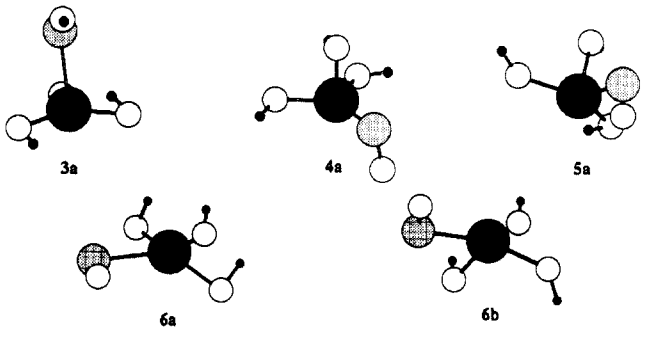

Figure 4. Structures and imaginary frequency displacement vectors (UHF/6-31G*) for selected isomers of **3**–**6**. Atomic sizes are arbitrary. Displacement vectors, originating at the indicated atoms and terminating at the small black spheres, are not shown if the terminatior point lies within the given atomic radius.

not. Instead the rotation coordinate continues to rise shallowly until the C_s **1d** is reached. Rather than eclipsing interactions, which are probably reduced in part due to the relatively long P–O bonds (compared to say C–O), the effect dominating the rotation coordinate appears to be of a different nature.

In a separate examination of the internal hydroxyl rotation in **7**, Gordon et al. performed a Fourier decomposition of the rotation coordinate to separate out dipole–dipole interactions, hyperconjugative interactions, and bond–bond repulsions.[23] They concluded in that case that hyperconjugative interactions dominated the rotaction coordinate. For **1**, however, this does not appear to be the case. Proceeding upward in energy, structural analysis indicates the dominant electronic effect involving oxygen to be improved P–O π bonding as greater overlap of the oxygen lone pairs with the singly occupied orbital occurs: the *r*PO bond length shortens from 1.723 Å for **1a** to 1.697 Å for **1d**. However, the dipole moment increases concomitantly, going from 1.242 D for **1a** to 2.134 D for **1d**. Indeed, after a small correction for bond–bond repulsive interactions, the rotation coordinate for **1** smoothly mimics a plot of dipole moment vs rotation angle. While this does not indicate that hyperconjugative interactions are absent, it does place severe limits on their angular dependence. The very small variations in P–H bond lengths in **1** provide some support for this analysis. Hence, **1b**, which not only has a small dipole moment but also minimizes bond–bond repulsions, emerges as the local minimum.

The rotation coordinate for **2**, on the other hand, is very similar to that obtained by Gordon et al. for **7**.[23a] It is apparent that the electron-accepting ability of the σ^*_{P-H} orbital is considerably improved for an axial hydrogen atom as opposed to an equatorial. This is unsurprising given the relatively higher energy of the σ_{P-H} bond orbital for the former compared to the latter. This conclusion enjoys structural support as well, with $r\mathrm{PH_a}$ being 1.480 Å when eclipsed by O–H and 1.452 Å when anti, these conformations allowing maximum and minimum hyperconjugative delocalization, respectively. Hence, for **2**, hyperconjugative interactions dominate the rotation coordinate,[24] and the local minimum, **2b**, is that isomer which enjoys maximum overlap of the oxygen lone pairs with an axial σ^*_{P-H} orbital.

In spite of arising from different effects, the magnitude of the overall rotation barriers appears not to be dramatically affected by the axial (4.6 kcal/mol) or equatorial (5.2 kcal/mol) nature of the hydroxyl group. For additional comparison, the pyramidal, closed-shell phosphinous acid, H_2POH, has been calculated at a similar level to have a barrier to hydroxyl rotation of 4.4 kcal/mol.[21d]

Pseudorotation Barriers. Vibrational analysis of the normal modes which are characterized by imaginary frequencies in **3** and **4** shows these structures, which result from some pseudorotational process that moves the unpaired electron from an equatorial position to an axial one, to be transition states for axial/equatorial hydrogen atom "exchange"[25] in **2** and **1**, respectively (Figure 4).

(23) (a) Schmidt, M. W.; Yabushita, S.; Gordon, M. S. *J. Phys. Chem.* **1984**, *88*, 382. (b) Radom, L.; Hehre, W. J.; Pople, J. A. *J. Am. Chem. Soc.* **1972**, *94*, 2371. (c) Veillard, A. *Chem. Phys. Lett.* **1969**, *1*, 51.

(24) These "anomeric" effects through second-row atoms, even with σ^*_{X-H}-type acceptor orbitals, are well documented; see: (a) Reed, A. E.; Schleyer, P. v. R. *J. Am. Chem. Soc.* **1987**, *109*, 7362, and references therein. (b) Denmark, S. E.; Cramer, C. J. *J. Org. Chem.* **1990**, *55*, 1806.

(25) We use "exchange" in the ensuing discussion in a purely topological sense, without respect to actual Cartesian coordinates. Thus, an axial and equatorial substituent are said to exchange if the axial moves to *some* equatorial site and the equatorial to *some* axial site while all other substituents remain topologically unchanged. In this particular molecule, site–site exchange with respect to *actual coordinates* may be achieved by a mirror reflection of the products of pseudorotation.

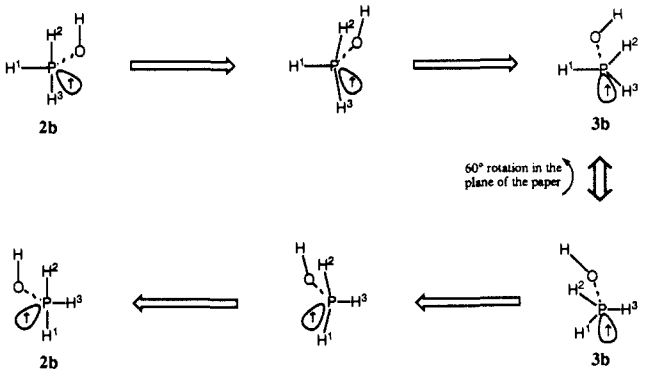

Figure 5. An example of a Berry-like pseudorotation exchanging two protons in **2b** via transition state **3b**. The intermediate structures may be viewed as square pyramids in which the unpaired electron occupies one of the basal positions.

Thus, **3a** is intermediate in the exchange of H_e with that H_a syn to the hydroxyl proton in **2b**, while in **3b** H_e exchanges with the H_a anti to that proton. These processes have activation barriers of 6.2 and 6.9 kcal/mol, respectively, *relative to* **2b**. Similarly, **4a** is intermediate in the exchange of H_a with that H_e gauche to the hydroxyl proton in **1b**, while in **4b** H_a exchanges with the H_e anti to that proton. In this case, the activation barriers are 4.3 and 9.0 kcal/mol, respectively. Given the mere 0.7 kcal/mol energy difference between **3a** and **3b**, it is likely that the majority of the energy difference between **4a** and **4b** is not due to eclipsing of the O–H and P–H_a bonds, but rather to oxygen lone pair/phosphorus unpaired electron interactions.

One of these exchange processes, **2b** → **3b** → **2b**, is illustrated in Figure 5, where the motion describes a Berry-like pseudorotation[26] with the singly occupied orbital part of the base of the square-pyramidal intermediate usually invoked as the Berry transition state. Since the unpaired electron cannot be explicitly localized, this is a somewhat arbitrary choice of convention, the turnstile mechanism of Ugi and Ramirez[27] for pseudorotation being topologically equivalent. The latter envisions holding one axial and one equatorial substituent locked while the remaining three rotate about the axis defined by all points mutually equidistant from them. In the transition state, it is assumed that this axis will also be the bisector of the angle defined by the two fixed substituents and the central atom. Howell and Olsen noted little difference in activation barrier heights when PH_4• was formally constrained to follow one or the other of these two pathways.[13b]

In both **3** and **4**, the unique exchange of two equivalent atoms to nonequivalent sites involves a single intermediate structure where those atoms are homotopic. In **1b** there are exactly two unique H_e with which H_a may exchange, and in **2b** there are exactly two unique H_a with which H_e may exchange. Hence, these four C_s structures with a single negative eigenvalue in their Hessian matrices potentially exhaust the set of H–H exchange transition states. Furthermore, in each case, the negative normal mode is of A″ symmetry, as expected for symmetric exchanges passing through C_s transition states.[28]

There remain two unique two-site exchange possibilities, each of which takes **1b** into **2b** reversibly. Since both of these local minima are of C_1 symmetry, the axial (equatorial) hydroxyl group may exchange with either of the two nonequivalent hydrogen atoms that are equatorially (axially) disposed. As the exchanging groups are nonequivalent as well, there is no a priori reason to expect intermediates having homotopic hydrogen atoms. Nevertheless, structures **5a** and **5b** do exhibit C_s symmetry, and their respective negative normal modes (which are of A′ symmetry, as expected for these *non*symmetric exchanges) may be followed to either local minimum. For these exchanges involving hydroxyl, the pseudorotation activation barriers are considerably higher, 17.0 and 18.8 kcal/mol relative to **1b** for **5a** and **5b**, respectively.

The tendency exhibited in the TBP_a structures **3**–**5** for the hydroxyl group to eclipse acceptor orbitals (which gives rise to the C_s symmetry in **5**) provides some indication of how important hyperconjugative effects are in describing the bonding in these TBP_a phosphoranyl species. Structural analysis provides insight into the relative degree to which delocalization occurs. The lengthening of the P–H bond on going from hydroxyl anti to eclipsed is 0.025 Å for **3**, 0.016 Å for **4**, and 0.015 Å for **5**.

It has been noted that pseudorotational barriers in phosphoranyl radicals tend to be higher than those found for the closed-shell phosphoranes.[2] For hydroxyphosphoranyl, the explanation is

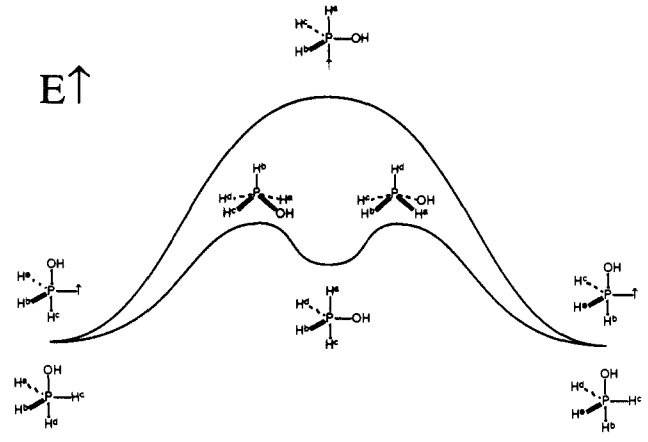

Figure 6. A potential surface comparing Berry pseudorotations for hydroxyphosphoranyl to hydroxyphosphorane. The TBP_a transition state for the former corresponds to a local minimum for the latter. The square-pyramidal transition states for pseudorotation of hydroxyphosphorane do not correspond to stationary points on the hydroxyphosphoranyl hypersurface.

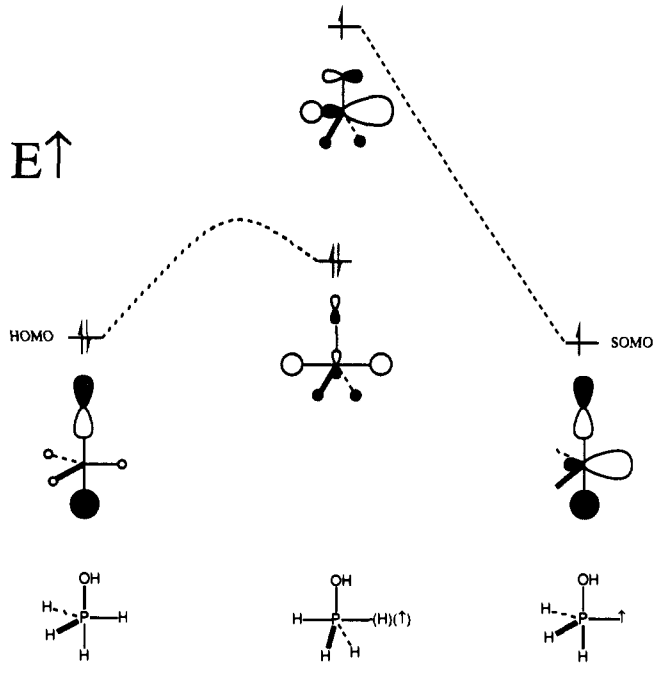

Figure 7. A qualitative description of the HOMO and SOMO for various isomers of hydroxyphosphorane and hydroxyphosphoranyl. These MOs were constructed from the 6-31G* molecular orbitals, ignoring the relatively minor contributions of the hydroxyl proton and heavy-atom d orbitals. No comparison of the absolute energies between the closed- and open-shell species is intended.

(26) Berry, R. S. *J. Chem. Phys.* **1960**, *32*, 933.
(27) Ugi, I.; Ramirez, F. *Chem. Br.* **1972**, *8*, 198.
(28) It is important to note, however, that there is no a priori requirement for these TBP_a structures to be saddle points (i.e., a square-pyramidal C_s structure similar to those found in phosphorane pseudorotations would as readily serve). By contrast, in unpublished work on the trihydroxyphosphoranyl radical, $HP(OH)_3$•, we have found that the C_{3v} TBP_a analogue to **4a** is not only a *local* minimum, it is only slightly higher in energy than the TBP_a *global* minimum.

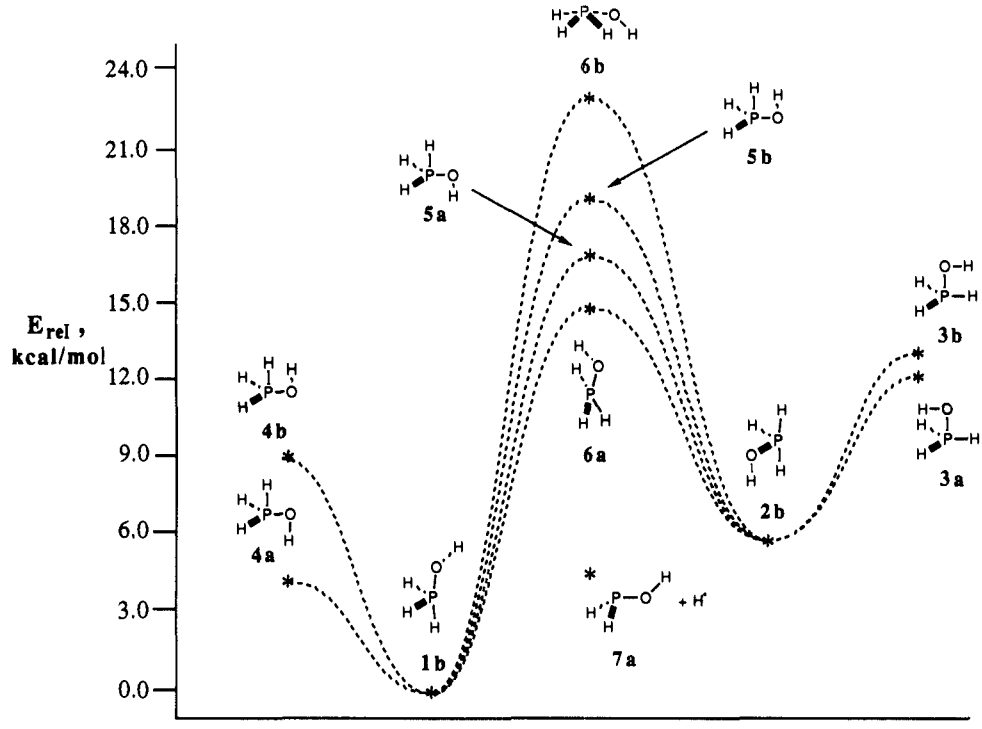

Figure 8. Relative energies and interconnecting pathways for all of the stationary points on the hydroxyphosphoranyl potential surface with Hessian matrices characterized by one or zero negative eigenvalues (saddle points from hydroxyl group rotation alone are not included). The infinitely separated pair of anti phosphinous acid and a hydrogen atom are included for reference.

provided by consideration of the molecular orbitals involved. In hydroxyphosphorane, replacement of the unpaired electron with a proton substituent renders the TBP_e **2** and TBP_a **4** (or **5**) equivalent. Thus, the phosphoranyl TBP_a transition states correspond to local minima for the phosphoranes (Figure 6). The question regarding comparison of barrier heights then becomes "Why is the hydroxyphosphorane local minimum of significantly lower relative energy than its hydroxyphosphoranyl TBP_a analogue?" Figure 7 presents a qualitative comparison of the SOMOs for **1** and **4** with the HOMOs for the axial and equatorial isomers of hydroxyphosphorane. The net overall effect of replacing the unpaired electron with a bonded substituent in the phosphorane is creation of a node at phosphorus in the HOMO, making this MO essentially the axial, nonbonding three-center four-electron orbital. The SOMO of the open-shell phosphoranyl species, on the other hand, is dominated by the hybridized p orbital containing the unpaired electron. While this orbital mixes in a *nonbonding* sense with the nonbonding 3c–4e orbital in the SOMO of the TBP_e radical, in the SOMO of the TBP_a species it represents the phosphorus contribution to the *two-center three-electron antibonding orbital* and additionally suffers a π-antibonding interaction with the oxygen p_z orbital. This accounts for the considerably higher energy of the TBP_a species over that of the TBP_e. A similar argument applies in the comparison of **2** and **3**.

A final point of interest is the greater similarity of structures **5** to **2b** than to **1b**; i.e., the large P–H_e bond lengths and wide angle between the homotopic hydrogen atoms and the short P–O bond length are all characteristic of those in **2**. This is to be compared with **4**, where the small H_e–P–H_e bond angle and intermediate length P–H_e bonds more closely resemble those in **1b**, from which **4** derives. Since **2b** is of higher energy than **1b**, the greater structural similarity of **5** to the former is in accord with the Hammond postulate (see Figures 4 and 8).[29]

Pseudoinversion Barriers. By consideration of hydroxyl rotation and phosphoranyl pseudorotation, all transition states for the exchange of any two substituents (to within enantiomerism) have potentially been found.[30,31] Given our topological definition of exchange,[25] these include as a subset all transition states that would more classically be considered to permute three substituents, since one such exchange must be degenerate in equatorial orientation. The only possible permutational processes remaining are those involving simultaneous exchange of both axial substituents with both equatorial. Such a process necessarily interconverts **1b** and **2b**.

Structure **6a** is the transition state for a pseudoinversion[32] that follows a pathway decreasing the angle between the two axial substituents while simultaneously increasing that between the two equatorial substituents (Figure 4). As noted above, there is no requirement for an intermediate connecting **1b** and **2b** to possess any symmetry, and indeed, **6a** does not. The large angles between each pair of "trans" substituents arise from repulsive interactions with the essentially pure p orbital containing the unpaired electron. The most remarkable feature of **6a** is that it lies only 14.9 kcal/mol above **1b**. Thus, *pseudoinversion is a lower energy pathway than pseudorotation to interconvert the two local minima for hydroxyphosphoranyl.*

(29) (a) Hammond, G. *J. Am. Chem. Soc.* **1955**, *77*, 334. (b) Farcasiu, A. *J. Chem. Educ.* **1975**, *52*, 76.

(30) This assumes, inter alia, that **1b** and **2b** are the only local minima. While it is not possible to map even a one-dimensional surface completely, the failure of extensive two- and three-dimensional searches conducted in an attempt to locate TBP_a local minima is sufficient for us to discount their existence for H_3POH^-.

(31) The trivial, high-energy process of hydroxyl inversion at oxygen is discounted. Other nonsymmetric transition states for such exchanges cannot be *rigorously* ruled out, but we seriously doubt their existence.

(32) Inversion is generally defined as a continuous deformation of a molecule or group such that each substituent on a central atom is translated through a common plane, along a path normal to the plane at the point of intersection. The final positions and the original are equidistant from the inversion plane, with each located uniquely in one of the two half-spaces defined by it (substituents in the plane remaining unchanged). In the conformational process for which **6a** is a transition state, only the unpaired electron is so translated; the atomic substituents remain in their respective half-spaces, albeit at different coordinates. In the process for which **6b** is a transition state, all of the substituents pass through a plane normal to the unpaired electron, but *not* from original positions to new ones equidistant from the inversion plane *nor* along paths normal to it at the point of intersection. Furthermore, the unpaired electron remains predominantly localized in the same half-space throughout. Hence, we refer to both of these processes as *pseudo*inversion.

(33) Cramer, C. J., unpublished calculations.

Table II. Selected Electronic Data for **1b** and **2b**[a]

structure	infrared frequencies,[b] cm^{-1}						μ, D
1b	281.1	620.6	639.5	794.0	1082.0	1137.9	1.3302
	1294.2	1336.7	2014.0	2682.6	2714.5	4091.7	
2b	466.9	798.2	870.3	957.5	971.4	1211.3	1.4742
	1252.2	1319.2	1858.2	2100.0	2647.7	4093.7	

[a] Calculated at the UHF/6-31G*//6-31G* level. [b] Uncorrected harmonic frequencies.

Structure **6b**, on the other hand, is the transition state for a pseudoinversion that follows a pathway bending the two axial substituents back, through a 180° angle, while expanding the angle between the two equatorial substituents (Figure 4). This is also exactly the structure expected for a Berry-like pseudorotation transition state where the unpaired electron acts as the apical substituent in the square pyramid (vide supra). Again, the intermediate exhibits no symmetry. This transition state has the highest energy of all of the located saddle points, lying 22.6 kcal/mol above **1b**.

Since **6a** and **6b** are C_1 structures that cover the two possible four-substituent exchange processes, i.e., inversion of the half-occupied orbital and its converse, there should be no remaining equilibrium structures with Hessians characterized by a single negative eigenvalue.[30,31]

Figure 8 shows the relative energy ordering for the various structures **1b**, **2b**, **3**–**6**, and **7a**, together with the sense in which they are interconnected. It is noteworthy that the hydroxyphosphoranyl global minimum lies 4.4 kcal/mol lower in energy than the separated phosphinous acid/hydrogen atom pair. This suggests that observation of hydroxyphosphoranyl under suitable conditions, e.g., matrix isolation, should be possible. Indeed, if there is a significant barrier to P–H bond homolysis,[15a] it might even be possible to observe some of the above listed conformational dynamics. As a potential aid to spectral identification, the uncorrected infrared frequencies calculated for **1b** and **2b** are collected in Table II. It is apparent that **1b** and **2b** should be easily distinguished. Fermi contact values, which may be useful in predicting isotropic hyperfine splittings, are presented in Table III and discussed below.

Electron Spin Resonance. Howell and Olsen[13b] in 1976 performed calculations on $PH_4^•$ at the 4-31G level. Their resulting C_{2v} TBP_e structure was characterized by long apical bonds and a SOMO dominated by the axial 3c–4e nonbonding orbital. The C_{3v} TBP_a structure ($\angle H_aPH_e$ constrained to 90°), conversely, had a short apical bond, long equatorial bonds, and a SOMO again P–H nonbonding, dominated by the *equatorial* hydrogen s orbitals. Although these results must be viewed with some skepticism, since the authors pointed out that at this level dissociation to PH_3 and H• occurs with no barrier, at the 6-311G** level the orbital compositions are qualitatively similar.[13c]

A later paper by Roberts[11] cited these results and added that if the bond lengths were reversed in the TBP_a radical, i.e., long apical, short equatorial, and *constrained at those lengths*, then the molecule adopts a C_{3v} geometry, which is essentially a distorted tetrahedron (DT) with a SOMO dominated by the apical hydrogen s orbital. This was offered as a model for phosphoranyl radicals of C_{3v} symmetry where the unpaired electron is assumed to reside in a $P–X_a$ antibonding orbital, a structure proposed for chlorotriphenylphosphoranyl (Chart I). Although MNDO calculations predict qualitatively similar SOMOs, they are unsatisfactory at reproducing ab initio relative energies.[14a] The assumption made, then, is that the magnitude of contribution made to the SOMO by a given atomic orbital will relate directly to the size of that atom's hfs (vide infra). Thus, based on the $PH_4^•$ model, the hfs for a given apical atom should be much larger in TBP_e structures than in corresponding TBP_a.

This lowest level paradigm remains to date the reference against which experimental hyperfine couplings are compared, in spite of the generally high degree of heteroatom substitution in the phosphoranyl radicals of experimental interest. Still more disturbing is that typically there is only a single measured hfs to compare, since a common substituent atom is the magnetically mute ^{16}O nucleus. It is perhaps not surprising then that various authors have claimed support for quite different geometries of the same molecule based on reference to this model, and that considerable controversy has arisen.

Prior to addressing individual cases, it is instructive to consider the various isomers of hydroxyphosphoranyl. For structures **1**–**6** the Fermi contact (FC) values are collected by atom in Table III. These are obtained from the SCF spin density matrix and the atomic orbitals and have been shown to correlate with isotropic hyperfine coupling constants.[13c,34,35] We are not concerned with the accurate prediction of hfs here, but rather with comparing the relative values that would be observed for various atoms at different geometries.

The first trend apparent in Table III is that the FC value for phosphorus is of little use in differentiating TBP_a from TBP_e—in each case it spans a range of ~0.4–0.9 au depending on the location and orientation of the hydroxyl group. There is apparently some relation between the magnitude of the FC value and the location of the hydroxyl group in each of the two structural possibilities, but specification on this basis would be tentative.

For oxygen, the FC value is relatively large in **1**, as expected for an axial substituent in a TBP_e geometry. However, it varies by 100% depending on the rotational isomer selected. Furthermore, although the FC values are very low in **2**, again as expected, in **3**, **4**, and **5b** they are comparable to or larger than those for **1**! For **3**, this is in especially sharp contrast to the predictions of the $PH_4^•$ model for axial substituents in a TBP_a phosphoranyl radical. It is evident that the SOMO for $PH_4^•$ is significantly perturbed when hydrogen is replaced by a second-row atom (e.g., compare the phosphoranyl TBP_a SOMO described above to that for **4** shown in Figure 7).

The hydrogen FC values, on the other hand, are entirely in harmony with the simple model system. Unfortunately, few phosphoranyl radicals substituted with hydrogen have been observed. Where observed, the experimental hfs is consistent with theory.[8a,e] There is apparently, however, some danger in assessing only the SOMO's AO composition when predicting hfs. Although the SOMO of **4** shows a large contribution from the s orbital of the axial hydrogen atom, nevertheless the Fermi contact term, which is a measure of spin density at the nucleus, is effectively zero.

The tendency, based on the $PH_4^•$ model, has been to assume that if a single substituent *must* reside in an apical position, then a large hfs indicates a DT, σ^*-type phosphoranyl radical as opposed to a TBP_a geometry. Thus Roberts[11] has disputed Hamerlinck, Schipper, and Buck's[10] assignment of **8** as a TBP_a radical,

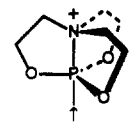

8

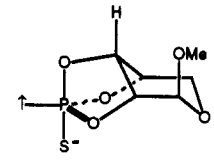

9

claiming that the observed 22.2-G hfs is similar to those from TBP_e structures in which nitrogen occupies an apical position, and thus too large for a TBP_a, nitrogen apical structure. Comparing the oxygen FC values of **1** and **3** in Table III indicates that such an argument by itself is probably inconclusive. For our own part, having examined numerous tetraheterosubstituted species we have

(34) The specific relation is $a_X^{iso} = (4\pi/3)g\beta\gamma_X(S_z)^{-1}\sum P_{\mu\nu}\phi_\mu(X)\phi_\nu(X)$ where the electronic g value is taken as 2.0, β is constant at 1.3996 MHz/G, γ_X is the magnetogyric ration of the nucleus of interest, $(S_z)^{-1} = 2.0$ for a doublet, and the summation term is the Fermi contact integral. See: Reference 13a.

(35) An alternative method correlates a_X^{iso} with total s-orbital spin density. This method has met with some criticism,[36] although in this instance it gives qualitatively similar results.

(36) Mackey, J. H.; Wood, D. E. *J. Chem. Phys.* **1970**, *52*, 4914.

Table III. Fermi Contact Values for Structures 1–6 Calculated at the 6-31G* Level

	Fermi contact value, au[a]								
		axial atoms				equatorial atoms			
structure	P	O[b]	H	H[b]	H[b]	O[b]	H	H[b]	H[b]
1a	0.792	0.172	0.092				−0.016	−0.016	
1b	0.804	0.194	0.088				−0.016	−0.015	
1c	0.705	0.317	0.083				−0.014	−0.012	
1d	0.976	0.393	0.105				−0.017	−0.017	
2a	0.466		0.106	0.106		0.036	−0.013		
2b	0.488		0.090	0.090		0.034	−0.014		
2c	0.485		0.104	0.104		−0.027	−0.013		
3a	0.312	0.197					0.066	0.027	0.027
3b	0.341	0.208					0.066	0.029	0.028
4a	0.823		−0.001			0.305	0.035	0.035	
4b	0.933		0.000			0.497	0.039	0.039	
5a	0.744		0.006			0.048	0.107	0.107	
5b	0.833		0.008			0.182	0.103	0.103	
6a[c]	0.183	0.213	0.002	−0.006	−0.010				
6b[c]	0.582	0.078	−0.008	−0.009	−0.010				

[a] $\hbar/2$ bohr^3. [b] Where data do not appear, this atom does not occupy such a position. [c] All substituents were arbitrarily defined as axial for **6**, since the axial–equatorial discriminator has little meaning for these geometries.

yet to find a phosphoranyl radical computationally predicted to prefer the DT, σ^* geometry over the analogous TBP_a structure ($\angle X_a$–P–Xe = 90° ± 3°).[33] We thus tend to accept the assertion of Hamerlinck, et al. in this instance.

In a related controversy, the TBP_e vs TBP_a geometry of the radical **9** has been called into question. Roberts[11] has argued that the 5-G hfs exhibited by the pseudoaxial ring proton indicates significant spin density on oxygen, which would not be expected for the TBP_a structure (which results from interchange of the sulfide anion with the unpaired electron in **9**) proposed by Hamerlinck et al.[10] We believe that the same caveat applies as illustrated above; however, in this instance we tend to side with Roberts. We have studied a variety of $XP(OH)_3^*$ phosphoranyl species with the O–H bonds constrained to lie along paths attached to an imaginary cyclohexyl ring; over the isoelectronic range of X substituents from F to BH_3^-, we find the TBP_e structure always to be of lower energy.[33]

While these arguments illustrate the danger of comparing complex phosphoranyl radicals to PH_4^*, we would not like to be seen as escaping the trap of the zeroth order only to fall into that of the first! Obviously the application of *this* model is limited as well. We maintain as a conservative rule, therefore, that in the absence of a *structure-specific* high-level theoretical treatment, or comparative data from other conformers of the same molecule, or hfs values from *several* atoms in the molecule, it is fruitless to assign geometry based solely on ESR data.

Conclusion. In summary, we have found that the hydroxyphosphoranyl radical is predicted at the ab initio level to exist in two trigonal-bipyramidal conformations. Both localize the unpaired electron equatorially, with the preferred isomer having the hydroxyl group disposed axially. Hydroxyl rotation barriers are subject to a variety of effects and are of similar energy to that for phosphinous acid. *Pseudorotations occur through transition states of TBP_a geometry, contrary to a proposal that such intermediates should be of DT, σ^*-type geometry.*[37] The activation barriers are in the range of 4–10 kcal/mol (for **1b** pseudorotation through **4a** has a lower barrier than does hydroxyl group rotation!) when only hydrogen atoms change relative positions and increase to 17–19 kcal/mol if the hydroxyl group does so as well. In addition, pseudoinversion through **6a**, *not pseudorotation*, was found to be the lowest energy pathway for interconverting the two local minima. Significant effects from inclusion of a single heteroatom on the localization of spin density in a phosphoranyl radical were noted.

Future work will focus on the effects of increased heteroatom substitution, methods for improving predicted isotropic hfs values, and elucidating the factors crucial to imparting stability to TBP_a structures.

Acknowledgment. Funding for this work was provided under projects 1C162622A553I and 1L161102A71A. I am grateful to Steve Lawhorne and the CRDEC Data Management Office for graciously providing Vax 11/780 time free of charge and to John Holter and Linda Stine for hardware technical assistance.

Supplementary Material Available: Cartesian coordinates, absolute energies, and unscaled frequencies for all stationary points at the UHF/6-31G* level (8 pages). Ordering information is given on any current masthead page.

(37) Giles, J. R. M.; Roberts, B. P. *J. Chem. Soc., Perkin Trans. 2* **1981**, 1211.